Nouman Amjed*, M. Naveed Aslam, Mazhar Hussain and Syed M. Qaim

Evaluation of nuclear reaction cross section data of proton and deuteron induced reactions on ^{75}As, with particular emphasis on the production of ^{73}Se

https://doi.org/10.1515/ract-2021-1018
Received February 18, 2021; accepted May 5, 2021;
published online May 21, 2021

Abstract: ^{75}Se ($T_{1/2}$ = 120 d), ^{73g}Se ($T_{1/2}$ = 7.1 h) and ^{72}Se ($T_{1/2}$ = 8.4 d) are important radioisotopes of selenium, being used in tracer studies, PET investigations and as a generator parent, respectively. Cross section data for the formation of those radionuclides in proton and deuteron induced reactions on ^{75}As were critically analyzed up to about 70 MeV. A well-developed evaluation methodology was applied to generate the statistically fitted cross sections, based on the critically analyzed literature experimental data and the theoretical cross section values of three nuclear model codes ALICE-IPPE, TAYLS 1.9, and EMPIRE 3.2. Using the fitted cross sections the integral yield of each radionuclide was calculated. For the estimation of impurities, the integral yield of each radionuclide was compared with the yields of the other two radionuclides over a given energy region, and therefrom the energy range was suggested for the high purity production of each of the radionuclides ^{75}Se, ^{73}Se and ^{72}Se. For production of the very important non-standard positron emitter ^{73}Se via the ^{75}As(p,3n)^{73}Se reaction, the optimum energy range was deduced to be E_p = 40 → 30 MeV, with a thick target yield of 1441 MBq/μAh and the ^{72,75}Se impurity level of <0.1%.

Keywords: nuclear data evaluation; nuclear model calculations; proton and deuteron induced reactions on ^{75}As; radionuclidic impurities; radionuclides ^{75}Se, ^{73}Se and ^{72}Se; thick target yield.

***Corresponding author: Nouman Amjed**, Division of Science and Technology, Department of Physics, University of Education, Lahore, Pakistan, E-mail: noumanamjad@ue.edu.pk
M. Naveed Aslam, Department of Physics, COMSATS University Islamabad, Lahore Campus, Lahore, 54000, Pakistan
Mazhar Hussain, Department of Physics, Government College University Lahore, Lahore, 54000, Pakistan
Syed M. Qaim, Institut für Neurowissenschaften und Medizin, INM-5: Nuklearchemie, Forschungszentrum Jülich GmbH, D-52425 Jülich, Germany

1 Introduction

Selenium is an essential element that plays a vital role in biological processes like formation of anti-oxidant defense and thyroid hormones, DNA synthesis, fertility and reproduction etc. [1]. Its radioisotopes can be applied to label physiological selenium compounds for tracer studies. Furthermore, selenium may serve as an analog to sulfur which itself has no suitable radionuclide for *in vivo* studies. This is important because sulfur is one of the main constituents of many pharmacologically relevant molecules.

Two radionuclides of selenium, namely ^{75}Se and ^{73}Se, are of special interest for organ imaging. The longer lived ^{75}Se ($T_{1/2}$ = 120 d) decays by electron capture (EC) and emits two γ-rays which are suitable for single photon emission computed tomography (SEPCT). However, the high radiation dose caused by it hinders its utilization in clinical practice [2, 3]. On the other hand, it is ideally suited for development work related to selenium separation [4] and preparation of labeled compounds [5, 6], as well as for the tracer studies related to selenium distribution and speciation in the environment. The other shorter lived radionuclide ^{73}Se ($T_{1/2}$ = 7.1 h) is a positron emitter and is very suitable for investigating slow metabolic processes via positron emission tomography (PET). The development of such longer lived metallic positron emitters, termed as "non-standard" positron emitters, is an active area of modern radiochemical research [7, 8] because many new medical applications are emerging which make use of those radionuclides. It may also be pointed out here that, besides the two radionuclides of selenium mentioned above, another radionuclide, namely ^{72}Se ($T_{1/2}$ = 8.4 d), is also of importance, not for direct use itself, but as a parent of the positron emitting ^{72}Se/^{72}As generator system [9–13]. The main decay data of the three radionuclides under consideration are listed in Table 1 (taken mainly from NuDat 2.8 [14]). Additionally, the data of the isomeric state ^{73m}Se are also given. It contributes partly to formation of ^{73g}Se (see below).

Table 1: Decay characteristics of ^{72}Se, ^{73m,g}Se and ^{75}Se.[a]

Radionuclide	Half-life $T_{1/2}$	Decay mode (%)	Main gamma ray energy (keV)	Abundance of γ-ray (%)
^{72}Se	8.4 d	EC (100)	45.8	58
^{73g}Se	7.1 h	β^+ (65.4) EC (34.6)	361.2	97.0
^{73m}Se	39.8 min	EC+ β^+ (27.4) IT (72.6)	253.7	2.36
^{75}Se	120 d	EC (100)	265.0	58.6

[a]Taken from NuDat 2.8 (NuDat 2.7) except for EC and β^+ branching values which were taken from Browne and Firestone , Table of radioactive isotopes. Wiley, New York.

For medium scale production of the three above mentioned radionuclides of selenium, viz. ^{75}Se, ^{73}Se and ^{72}Se, use has been made of ^{3}He- and α-particle induced reactions on germanium [11, 15–17], proton and deuteron induced reactions on arsenic [4, 18–21] and high-energy induced reactions on bromine [12, 22]. All aspects of development work, namely nuclear data, targetry, chemical processing and quality control of the product, have been described in the literature. In this study, however, we limit ourselves to the analysis and standardization of cross sections of proton and deuteron induced reactions on ^{75}As [13, 18, 19, 23–30].

The aim of this work is to provide evaluated and reliable data for the production of each of the three above mentioned radionuclides with highest possible yield and the minimum radionuclidic impurity [31, 32]. The main emphasis is, however, on data for ^{73}Se. Some attempts at the systematization of the excitation functions of the reactions leading to the production of ^{73}Se were reported earlier [33, 34]. Very recently the data of the reaction ^{75}As(p,3n)^{73}Se were evaluated under a Co-ordinated Research Project (CRP) of the IAEA [35]. The methodology used in that work was, however, different than in our work. Those authors used a statistical approach to select the concordant set of experimental data and then a Pàde fitting was done to obtain the recommended excitation function. We applied a theory-aided procedure to select the data and then the fitting was performed by a polynomial function. We compare and discuss our results with those reported in the IAEA evaluation. On the other hand, it should be mentioned that no evaluation of the reactions leading to the formation of ^{75}Se and ^{72}Se was presented in the CRP report [35]. Our study on those reactions should therefore help to optimize the production of each of the three radionuclides.

2 Compilation and normalization of data, nuclear model calculations and evaluation methodology

2.1 Compilation and normalization

The main decay data of the radionuclides under consideration are given in Table 1. They were mostly taken from the Nudat 2.8 database. All experimental data reported on the production of ^{73}Se, ^{72}Se and ^{75}Se in proton and deuteron induced reactions, namely ^{75}As(p,3n)^{73}Se, ^{75}As(p,4n)^{72}Se, ^{75}As(p,n)^{75}Se, ^{75}As(d,4n)^{73}Se, ^{75}As(d,5n)^{72}Se and ^{75}As(d,2n)^{75}Se were compiled. The *Q*-values, threshold energies and the references are given in Table 2. The decay data, i.e., half-life, gamma ray energies and intensities reported in all the experiments were compared with the standard values (cf. Table 1). The normalization of the decay data was performed according to their differences from the standard values [14]. In most of the reported experiments authors used a Faraday cup and monitor reactions to determine the charged particle beam before and within the stacked target. All the reported monitor reaction data were compared with the charged particle monitor reaction database of the IAEA [36], and normalizations were performed in case of significant differences.

Initially the results of TENDL library were used to check the consistency of the experimental data, but later the reliability of the data was checked with the results of detailed nuclear model calculations.

2.2 Calculations using ALICE-IPPE, TALYS 1.9 and EMPIRE 3.2

To check the uniformity and reliability of the experimental data, three nuclear model calculations with well-established nuclear model codes, namely ALICE-IPPE, TALYS 1.9 and EMPIRE 3.2 were performed. Different input parameters [37] were adjusted within their recommended limits to get an agreement between theoretical and experimental data [38, 39].

The ALICE-IPPE [40] is based on purely evaporation formalism, with the limitation that it can only calculate the total production cross section. The ALICE code cannot calculate the cross sections for the isomeric states. In comparison, EMPIRE and TALYS are modern nuclear model codes and are flexible with regard to the selection of different optical models and their parameters [41–45].

Table 2: Investigated nuclear reactions for the formation of ^{72}Se, ^{73m,g}Se with their *Q* values, threshold energies and references.

Nuclear reaction	*Q*-value (MeV)	Threshold energy (MeV)	References
^{75}As(p,3n)^{73}Se	−21.73	22.02	Brodovitch et al. [23], Mushtaq et al. [19], Qaim et al. [24], Levkovskij [25], Nozaki et al. [18]
^{75}As(p,3n)^{73m}Se	−21. 76	22.05	Qaim et al. [24]
^{75}As(p,4n)^{72}Se	−30.16	30.56	Mushtaq et al. [19], DeGraffenreid et al. [13], Nozaki et al. [18]
^{75}As(p,n)^{75}Se	−1.64	1.66	Albert [26], Delaunay-Olkowsky et al. [27], Johnson et al. [28], Johnson et al. [29], Brodovitch et al. [23], Mushtaq et al. [19], Levkovskij [25], DeGraffenreid et al. [13], Nozaki et al. [18]
^{75}As(d,4n)^{73}Se	−23.90	24.60	Röhm and Münzel [30], Mushtaq et al. [19], Qaim et al. [24]
^{75}As(d,4n)^{73m}Se	−23.93	24.63	Qaim et al. [24]
^{75}As(d,5n)^{72}Se	−32.38	33.25	Röhm and Münzel [30], Mushtaq et al. [19],
^{75}As(d,2n)^{75}Se	−3.87	3.97	Röhm and Münzel [30], Mushtaq et al. [19],

Furthermore, cross sections for the isomeric states can also be calculated. So, one can expect better theoretical predictions for the reported experimental data.

2.3 Evaluation methodology

For the evaluation of experimental data, a well-developed evaluation methodology was used [38, 39]. It consists of two steps; first, to check the consistency in the data using a nuclear model calculation, second, to fit the selected data using a polynomial function. Thus, the ratio of measured data to a nuclear model calculation ($\sigma_{meas}/\sigma_{model}$) was obtained and polynomial fitting was performed. In the fitting process, the measured data points away from 3σ limit of the fitting curve were eliminated. The polynomial fitting was then performed again for the remaining data. The evaluated cross section ($\sigma_{evaluated}$) was derived from the energy-dependent normalization factor $f(E)$ and the model calculated cross section $\sigma_{model}(E)$, such that

$$\sigma_{evaluated} = f(E)\sigma_{model}(E)$$

While performing polynomial fitting, experimental uncertainties were also considered and plotted with fitted data as 95% upper/lower confidence limits. This evaluation procedure was recapitulated with all three model calculations to generate the fitted cross sections. Then the recommended cross sections for the reaction were obtained by taking the averages of the three normalized/fitted cross sections.

It should be noted that, despite the allowable variances in the input parameters, we were unable to achieve a fair agreement between experimental data and model calculation for a few nuclear reactions. In those instances, we only performed a polynomial fitting through the experimental data.

3 Evaluation of production data of ^{73}Se, ^{72}Se and ^{75}Se in proton induced reactions on ^{75}As

3.1 ^{75}As(p,3n)^{73}Se reaction

The database of this reaction is good; five groups reported experimental cross sections for this reaction. The normalized literature data along with the results of the three nuclear model calculations (namely ALICE-IPPE, TALYS 1.9 and EMPIRE 3.2) are shown in Figure 1. The results by Levkovskij (1991) [25] were normalized by a factor of 0.75, as suggested by Qaim et al. (2014) [46], based on an analysis of the monitor reaction used by

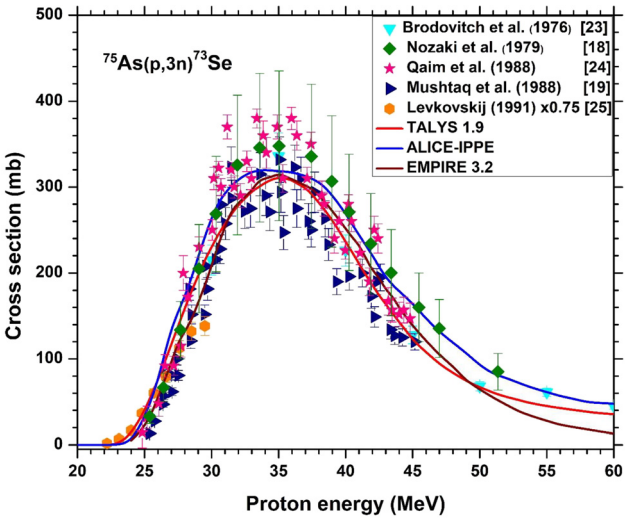

Figure 1: Normalized experimental data and results of nuclear model calculations for the ^{75}As(p,3n)^{73}Se reaction.

Levkovskij. A similar correction value was suggested by Hermanne et al. [36].

All normalized cross sections [18, 19, 23–25], except those by Qaim et al. [24] given in EXFOR are consistent with one another and also with the results of nuclear model calculations TALYS and EMPIRE, but ALICE-IPPE values slightly overestimate the experimental excitation function beyond 38 MeV. The TENDL results (not shown in Figure 1) were also more or less in agreement up to 30 MeV but showed large deviations at higher energies. It should be pointed out here that out of the five groups mentioned above, four [18, 19, 23, 25] measured the cumulative cross section for the formation of ^{73g}Se, i.e. the sum of its direct formation and some decay contribution from the short-lived ^{73m}Se. Qaim et al. [24], on the other hand, measured the isomeric cross-section ratio of ^{73m,g}Se, and therefrom estimated the total fraction of ^{73m}Se decaying to ^{73}As rather than to ^{73g}Se. Thus, they got the total cross section for the ^{75}As(p,3n)$^{73m+g}$Se channel. Those data are more relevant to the fundamental understanding of the isomer distribution in the pair ^{73m}Se/^{73g}Se. For the practical application to the production of ^{73g}Se, they are not comparable to the other data. The entry in the EXFOR was thus misleading. It has been corrected in the meantime. In our evaluation we therefore did not consider them further.

As the next step, the above-described theory-aided evaluation methodology was applied to obtain the ratio of the experimental data to the theoretical results by the EMPIRE 3.2 code which was then plotted as a function of proton energy with 95% confidence limits (Figure 2). The data points that showed deviation beyond 3σ limits were deselected, and then the polynomial fitting of data was

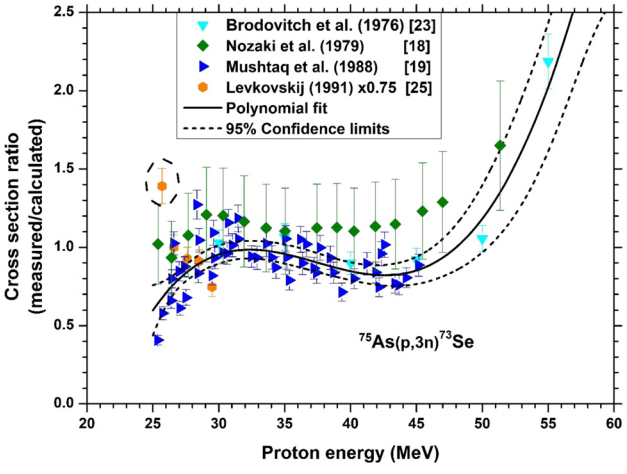

Figure 2: Ratio of measured cross section to calculated cross section by EMPIRE, plotted as a function of proton energy.

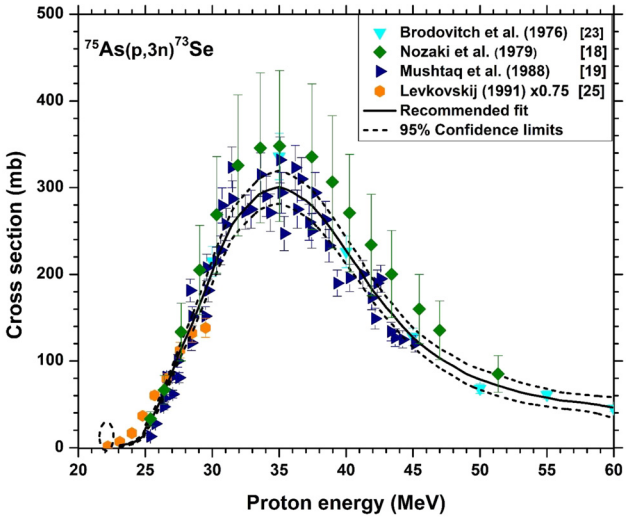

Figure 3: Recommended cross section curve with 95% upper and lower confidence limits for the ^{75}As(p,3n)^{73}Se reaction; the encircled data points were neglected.

repeated. The polynomial fit obtained was multiplied by the EMPIRE 3.2 data to produce normalized EMPIRE 3.2 values for the whole excitation function. The same procedure was repeated to obtain normalized values also by the ALICE-IPPE and TALYS 1.9.

The recommended cross sections were then generated by averaging all three normalized values from the three calculational codes. The recommended curve with 95% confidence limits together with the selected experimental data is shown in Figure 3, whereby the encircled points show the deselected values. Numerical values of the recommended fit with 95% confidence limits are given in Table 3.

3.2 ^{75}As(p,4n)^{72}Se reaction

For this reaction, three experiments were found in the literature [13, 18, 19]. The reported data are consistent with one another. The experimental data along with the results of nuclear model calculations are shown in Figure 4. Up to 45 MeV the results of EMPIRE, ALICE-IPPE and TALYS are in fair agreement with the experimental data but at higher energies EMPIRE and TALYS underestimate the excitation function whereas ALICE-IPPE fails to explain the trend of the excitation function. The TENDL results (not given in Figure 4) showed no agreement over the whole excitation function. The recommended cross sections were obtained using the polynomial fit of the experimental data (Figure 4); the numerical values are given in Table 3.

Table 3: Recommended cross sections for the formation of ^{75}Se, ^{73g}Se and ^{75}Se in proton-induced reactions on ^{75}As.

Energy (MeV)	^{75}As(p,n)^{75}Se			^{75}As(p,3n)^{73g}Se			^{75}As(p,4n)^{72}Se		
	Cross section (mb)	95% confidence limits		Cross section (mb)	95% confidence limits		Cross section (mb)	95% confidence limits	
		Lower	Upper		Lower	Upper		Lower	Upper
4	64	46	81						
5	146	127	165						
6	258	230	286						
7	387	350	424						
8	513	473	553						
10	665	622	707						
12	607	564	649						
14	410	363	456						
16	234	187	280						
18	123	75	179						
20	82	60	104						
22	57	47	67						
24	42	34	50	5	4	7			
25	38	30	46	22	18	26			
26	35	27	43	50	44	56			
28	32	25	39	125	117	134			
29	32	26	39	163	152	174			
30	33	26	39	203	189	217			
31	33	26	40	241	226	257			
32	34	27	41	268	251	285			
33	35	27	42	284	267	302			
36	36	28	43	295	276	314	3	2	3
37	35	28	43	285	266	304	6	5	7
38	35	27	42	269	252	287	12	11	13
39	34	26	42	249	233	266	20	18	21
40	33	25	41	227	212	242	31	29	33
41	32	24	40	206	192	220	42	39	45
42	30	22	38	181	168	194	51	47	55
43	28	19	37	162	150	174	60	55	66
44	26	17	36	144	132	156	66	58	73
45	24	14	35	127	116	138	76	67	85
47	20	9	32	103	92	114	91	81	101
48	19	7	30	94	83	106	97	85	109
50	15	2	28	79	67	91	104	90	118
51	14	1	27	73	61	85	105	91	120
54	11	4	26	60	50	71	104	90	118
57	11	7	30	53	44	62	98	85	110
60	13	0.2	32	46	34	58	88	77	99
65	11	0.1	28	26	25	30	85	80	90
70	7	0.1	7	22	20	24	80	76	84

3.3 ^{75}As(p,n)^{75}Se reaction

The database of this reaction is fairly strong; 10 groups measured cross sections for the production of ^{75}Se using this reaction (see Table 2). All the normalized experimental data along with the results of nuclear model calculations by ALICE-IPPE, TALYS 1.9 and EMPIRE 3.2 are shown in Figure 5. All literature data and nuclear model calculations are consistent with one another within the limits of their uncertainties. Also the TENDL values (not shown in Figure 5)

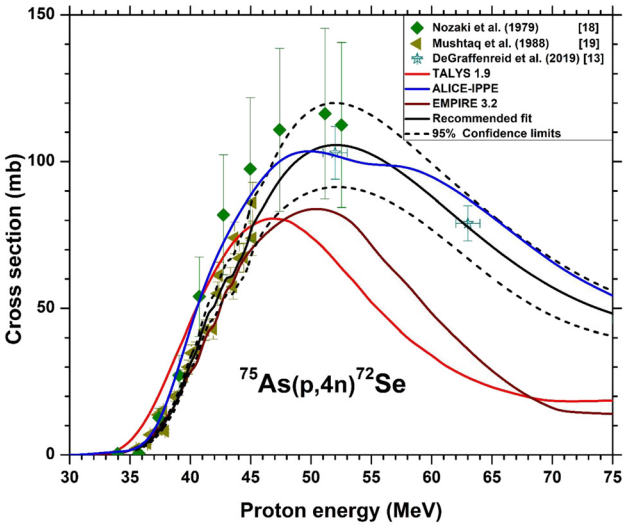

Figure 4: Normalized experimental data and results of nuclear model calculations along with the recommended cross section curve with 95% upper and lower confidence limits for the ^{75}As(p,4n)^{72}Se reaction.

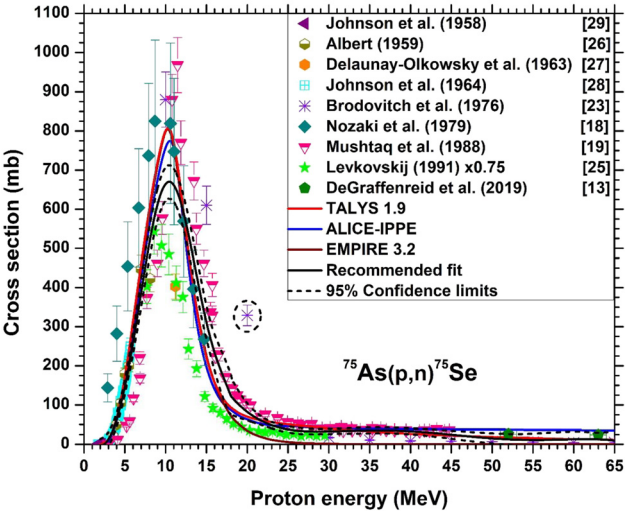

Figure 5: Normalized experimental data and results of nuclear model calculations along with the recommended cross section curve with 95% upper and lower confidence limits for the ^{75}As(p,n)^{75}Se reaction; the encircled data points were neglected.

agree. Only the results reported by Mushtaq et al. [19] and Nozaki et al. [18] are somewhat higher than the other values. The shape of all the theoretical excitation functions is similar to the experimental results; however, they slightly overestimate the cross section in the peak region. The above-mentioned evaluation methodology was employed to obtain the recommended curve with 95% confidence limits (Figure 5). The numerical values are given in Table 3.

4 Evaluation of production data of ^{73}Se, ^{72}Se and ^{75}Se in deuteron-induced reactions on ^{75}As

4.1 ^{75}As(d,4n)^{73}Se reaction

The database of this reaction is fair; three experiments have been reported in the literature (Table 2). Figure 6 shows the normalized literature data along with the results of the three nuclear model calculations, i.e. TALYS 1.9, EMPIRE 3.2 and ALICE-IPPE. Similar to the (p,3n) reaction discussed above, the results by Qaim et al. [24] given in EXFOR are shown in this diagram but not treated further in the evaluation process. The experimental values show consistency with one another up to 40 MeV; however, after this energy the experimental values by Röhm and Münzel are very low. A comparison of experimental data with theoretical nuclear model calculations shows that EMPIRE and TALYS are consistent with each other and with the experimental data but after 50 MeV, TALYS overestimates the experimental values. The results of ALICE-IPPE and values from TENDL library (not shown in Figure 6), are in agreement with the experimental results up to 39 MeV; thereafter, they slightly underestimate the cross section up to 50 MeV. On the whole, the shapes of excitation functions based on experimental data and theoretical results from nuclear model codes are rather similar.

Figure 7 shows the recommended curve with 95% confidence limits, with the deselected values encircled. The recommended cross sections were obtained by taking

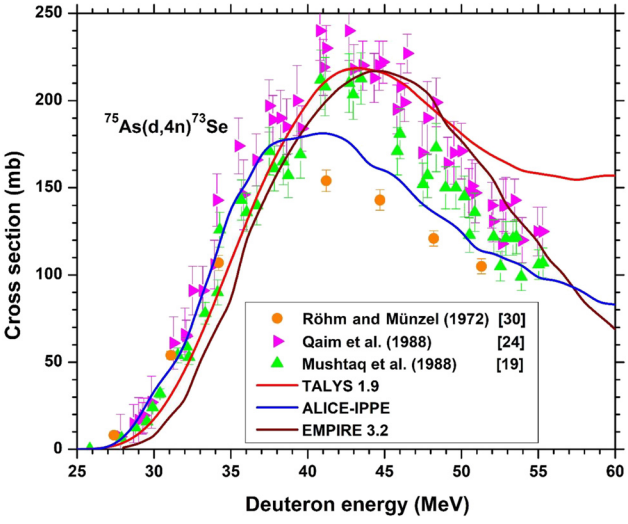

Figure 6: Normalized experimental data and results of nuclear model calculations for the ^{75}As(d,4n)^{73}Se reaction.

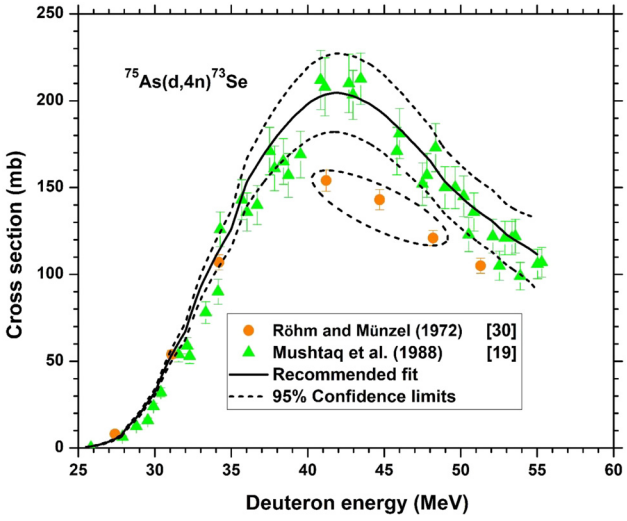

Figure 7: Recommended cross section curve with 95% upper and lower confidence limits for the ^{75}As(d,4n)^{73}Se reaction; the encircled data points were neglected.

an average of normalized values of TALYS 1.9 and EMPIRE 3.2. Table 4 provides numerical values of the recommended fit with 95% confidence limits.

4.2 ^{75}As(d,5n)^{72}Se reaction

Only two groups of authors, namely Mushtaq et al. [19] and Röhm and Münzel [30] reported measurements for this reaction. Those measurements are in agreement with each other. Figure 8 shows the normalized experimental data along with the results of the nuclear model calculations. The results of ALICE-IPPE and TALYS 1.9 are in agreement with the experimental data. EMPIRE results underestimate the cross section. The TENDL data (not shown in Figure 8) were very discrepant. The above-mentioned evaluation methodology was used to generate the recommended cross sections. The numerical values are given in Table 4.

Table 4: Recommended cross sections for the formation of ^{75}Se, ^{73g}Se and ^{72}Se in deuteron-induced reactions on ^{75}As.

Energy (MeV)	^{75}As(d,2n)^{75}Se			^{75}As(d,4n)^{73g}Se			^{75}As(d,5n)^{72}Se		
	Cross section (mb)	95% confidence limits		Cross section (mb)	95% confidence limits		Cross section (mb)	95% confidence limits	
		Lower	Upper		Lower	Upper		Lower	Upper
6	29	27	32						
7	58	55	60						
8	72	70	74						
9	92	89	94						
10	125	123	127						
11	174	172	176						
13	303	301	305						
15	434	432	437						
17	527	525	529						
19	557	555	559						
21	526	524	529						
23	451	448	453						
25	355	352	357	0	0	0			
27	262	260	264	4	3	4			
28	222	220	225	10	9	11			
29	189	187	192	20	18	21			
30	163	160	165	32	30	34			
31	143	141	146	52	49	56			
32	130	127	132	67	62	72			
33	122	119	124	93	86	100			
34	117	115	120	111	102	120			
35	116	113	119	126	116	137			
36	116	113	119	153	139	167			
37	115	112	119	167	152	183			
38	114	111	118	180	162	198			
39	112	109	115	190	171	209	1	1	1
40	108	105	111	198	177	219	2	2	2
41	102	99	105	203	181	225	3	3	3

Table 4: (continued)

Energy (MeV)	^{75}As(d,2n)^{75}Se			^{75}As(d,4n)^{73g}Se			^{75}As(d,5n)^{72}Se		
	Cross section (mb)	95% confidence limits		Cross section (mb)	95% confidence limits		Cross section (mb)	95% confidence limits	
		Lower	Upper		Lower	Upper		Lower	Upper
42	95	92	99	205	182	227	5	5	6
43	88	85	92	203	180	225	8	8	9
44	81	78	85	198	176	221	11	11	12
45	76	72	80	192	170	215	15	14	15
46	72	69	76	184	162	206	18	17	19
47	71	67	75	175	154	196	22	21	24
48	71	67	75	165	146	185	27	25	28
49	73	69	77	153	134	172	32	30	33
50	74	70	79	145	127	163	36	34	39
51	75	70	79	137	119	155	40	38	43
52	73	68	77	131	113	149	43	40	46
53	68	63	72	123	105	140	45	42	49
54	62	57	67	117	99	136	49	45	54
55	61	56	65	112	91	132	1	1	1

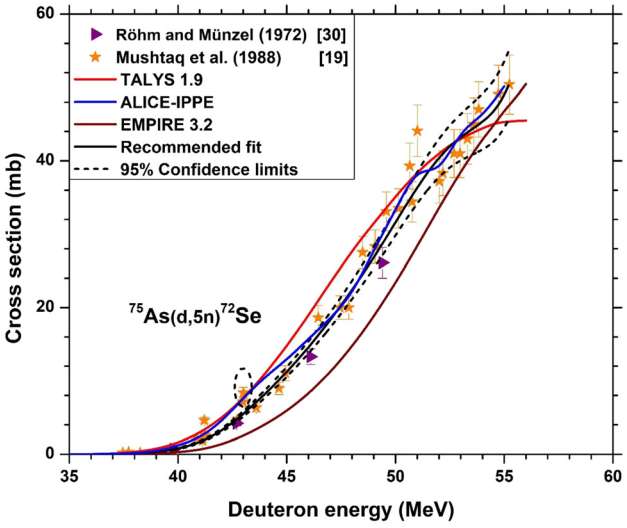

Figure 8: Normalized experimental data and results of nuclear model calculations along with the recommended cross section curve with 95% upper and lower confidence limits for the ^{75}As(d,5n)^{72}Se reaction; the encircled data points were neglected.

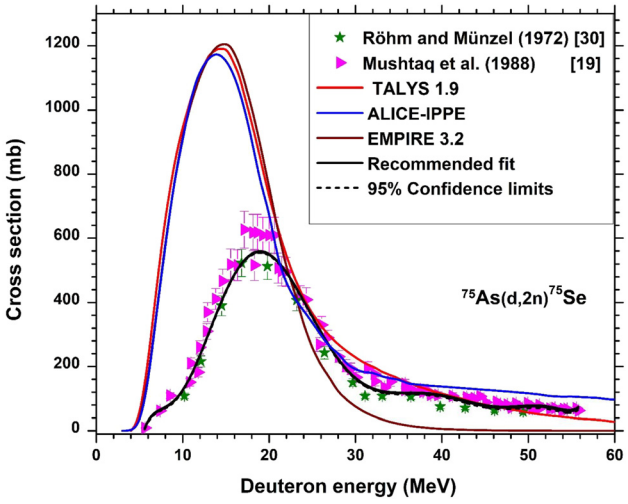

Figure 9: Normalized experimental data and results of nuclear model calculations along with the recommended cross section curve with 95% upper and lower confidence limits for the ^{75}As(d,2n)^{75}Se reaction.

4.3 ^{75}As(d,2n)^{75}Se reaction

For this reaction only two experiments were found in the literature (see Table 2) [19, 30]. Normalized data along with the results of nuclear model calculations are shown in Figure 9. Both experiments are in good agreement with each other. The results of all nuclear model calculations are consistent with one another but they are not in agreement with the experimental data. The trend of the excitation function given by the nuclear model calculations is completely different from the experimental curve. This is typical of some deuteron induced reactions where the model calculation is often not able to describe the experimental cross section, mainly due to the neglect of the deuteron breakup process. Therefore, in this case, we relied only on the experimental data, and polynomial fitting was done to generate the recommended cross sections (see Figure 9). The numerical values are given in Table 4.

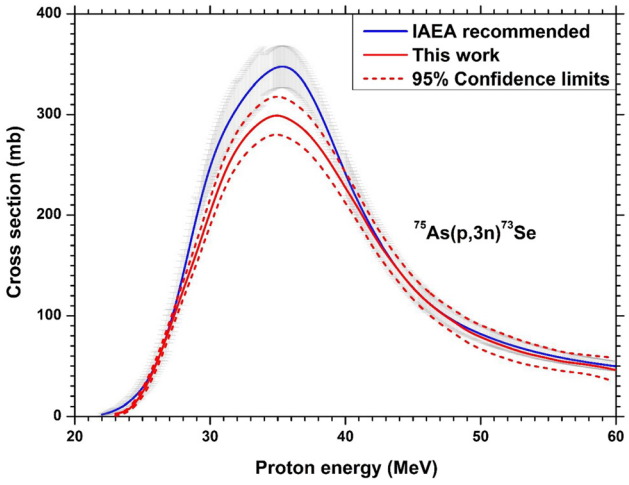

Figure 10: Comparison of present evaluated curve with that of the IAEA CRP curve for ^{75}As(p,3n)^{73}Se reaction.

5 Comparison of present evaluation with earlier evaluation of ^{73}Se production data

In the Coordinated Research Project (CRP) of the IAEA, only the main route for the production of ^{73}Se, namely the ^{75}As(p,3n)^{73}Se reaction, was studied [35]. In that work the selection of experimental data was based solely on statistical fitting considerations, and a Pade fitting was done, deducing the region-wise percentage uncertainty. Many data were rejected and the evaluation beyond 30 MeV was based only on the data by Brodovitch et al. [23] and Qaim et al. [24] given in EXFOR. A comparison of our evaluated curve with that of the CRP curve [35] is shown in Figure 10. Evidently, the CRP result is much higher. We believe, that our choice of experimental data (or their rejection) is based on a more scientific and rigorous analysis.

For the ^{75}As(d,4n)^{73}Se reaction no previous evaluation has been reported; any comparison is therefore not possible. Similarly, data for the formation of ^{72}Se and ^{75}Se both in proton and deuteron induced reactions on ^{75}As were previously not evaluated.

6 Calculation and comparison of integral yields

Recommended cross sections for all reactions were utilized to calculate the integral yields of the products using the known formula [47], assuming a beam current of 1 μA and an irradiation time of 1 h [48]. The results are discussed below.

6.1 Integral yields of ^{75}As(p,3n)^{73}Se, ^{75}As(p,4n)^{72}Se and ^{75}As(p,n)^{75}Se reaction products

The calculated integral target yields of ^{75}As(p,3n)^{73}Se, ^{75}As(p,4n)^{72}Se and ^{75}As(p,n)^{75}Se reactions along with the experimental values at low-current irradiations reported by Nozaki et al. [18], Dmitriev [49] and Rowshanfarzad et al. [50] are shown in Figure 11. For the reaction ^{75}As(p,3n)^{73}Se, the reported literature yields are in good agreement with our calculated integral yields. However, the yield value reported by Rowshanfarzad et al. [50] at 30 MeV is lower than our calculated yield. In case of ^{75}As(p,n)^{75}Se reaction the values reported by Dmitriev [49] are lower than our calculated yield values. The shaded areas depict the optimum energy ranges for the production of ^{75}Se and ^{73}Se. The energy beyond 50 MeV is suitable for the production of ^{72}Se. The optimum energy ranges deduced for the production of the three above mentioned selenium radionuclides in proton induced reactions on arsenic are given in Table 5, together with the calculated thick target yield of the desired radionuclide as well as the levels of the relevant impurities. The data for ^{73}Se are in agreement with the calculated values by Mushtaq et al. [19], Königs et al. [4] as well as by Qaim and Spahn [33]. Important is also to mention that the yield calculated from the CRP curve (Tarkanyi et al. [35]) is only about 3% higher than our value, despite their higher cross section in the peak area. Production data on ^{73}Se using beam currents of 2–7 μA are also available [4, 19–21].

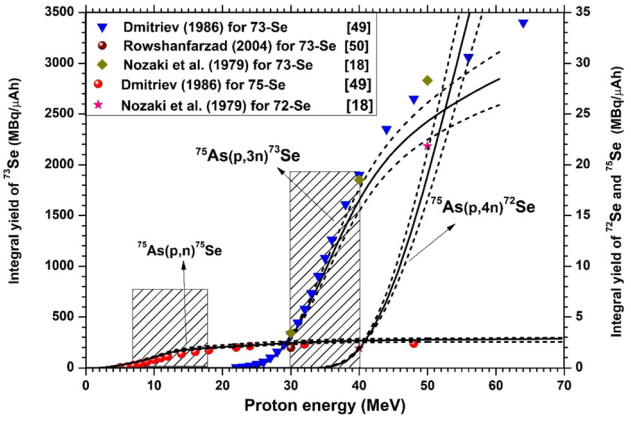

Figure 11: Calculated integral yields of ^{75,73,72}Se via the ^{75}As(p,n)^{75}Se, ^{75}As(p,3n)^{73}Se and ^{75}As(p,4n)^{72}Se reactions for 1 h irradiations. The shaded areas give suitable energy ranges for the production of ^{75}Se and ^{73}Se. Some measured yields are also shown.

Table 5: Optimized energy range with calculated thick target yield of the desired radionuclide and percentage level of the radionuclidic impurity ^{72}Se and ^{75}Se.

Radionuclide	Nuclear reaction	Energy range (MeV)	Thick target yield at EOB[a] (MBq/μAh)	Radionuclidic impurity at EOB (%)	
				Calculated	Experimental
^{73}Se	^{75}As(p,3n)	40 → 30	1441.3	^{72}Se (0.086); ^{75}Se (0.014)	^{72}Se (0.1); ^{75}Se (0.03)[b]
	^{75}As(d,4n)	45 → 33	715.1	^{72}Se (0.052); ^{75}Se (0.14)	^{72}Se (0.1); ^{75}Se (0.2)[b]
^{75}Se	^{75}As(p,n)	18 → 7	1.65	None	None[c]
	^{75}As(d,2n)	25 → 12	2.72	None	d)
^{72}Se	^{75}As(p,4n)	60 → 45	38.3	^{75}Se (0.12); ^{73}Se[e]	^{75}Se (<5.0)[f] [d]
	^{75}As(d,5n)	45 → 33	0.37	^{75}Se (260.2); ^{73}Se[e]	[d] [d]

[a]Calculated from the recommended excitation function, assuming an irradiation time of 1 h at a beam current of 1 μA. [b]Measured by Mushtaq et al. [19]. [c]Investigated by Blessing et al. [21]. [d]Not measured. [e]^{73}Se level at EOB is more than 100 times higher, but it becomes negligible after a decay period of about 2 days. [f]Measured by DeGraffenreid et al. [11] after long irradiations.

The experimental yield corresponds to about 70% of the theoretical yield. Considering the various factors involved, e.g. inhomogeneity in the beam, radiation damage effects, loss in chemical processing etc. [51], this yield value is acceptable. More important is the ratio of the impurity to the yield of the desired radionuclide, which is independent of the irradiation conditions. Experimentally, those ratios were found to be approximately in agreement with the theoretical values (cf. Table 5). Also for ^{75}Se production, experiments with beam currents up to 25 μA were done [21]. As expected, the experimental yield was again about 70% of the theoretical value and no impurity was detected. With regard to ^{72}Se, high current experiments with beams of up to 165 μA gave experimental yield and the ^{75}Se/^{72}Se impurity ratio [13]. In general, the evaluated/recommended cross section data reported in this work for the three radionuclides appear to be supported by the results of the various production experiments. For exact validation, however, integral yields using well-planned low current benchmark experiments need to be measured.

6.2 Integral yields of ^{75}As(d,4n)^{73}Se, ^{75}As(d,5n)^{72}Se and ^{75}As(d,2n)^{75}Se reaction products

Using the recommended cross sections, integral yields for the ^{75}As(d,4n)^{73}Se, ^{75}As(d,5n)^{72}Se and ^{75}As(d,2n)^{75}Se reaction products were calculated and the results are given in Figure 12 along with the reported values by Dmitriev [49]. For the ^{75}As(d,4n)^{73}Se reaction our calculated values are higher than those reported by Dmitriev [49], but for

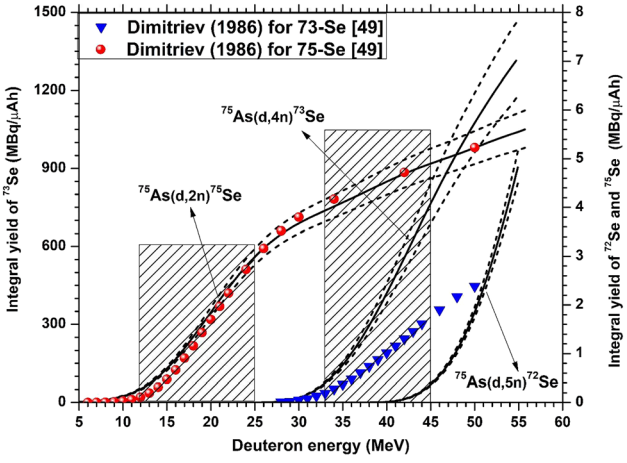

Figure 12: Calculated integral yields of ^{75,73,72}Se via the ^{75}As(d,2n)^{75}Se, ^{75}As(d,4n)^{73}Se and ^{75}As(d,5n)^{72}Se reactions for 1 h irradiations. The shaded areas give suitable energy ranges for the production of ^{75}Se and ^{73}Se. Some measured yields are also shown.

^{75}As(d,2n)^{75}Se reaction Dmitriev values [49] are in agreement with our calculated values. The shaded areas give the suitable energy ranges for the production of ^{75}Se and ^{73}Se.

Similar to proton induced reactions on ^{75}As described above, the suitable energy ranges deduced for the production of the three selenium radionuclides in deuteron induced reactions on ^{75}As are also given in Table 5, together with the calculated thick target yields and the levels of impurities. The data for ^{73}Se are in agreement with the calculated values given by Kőnigs et al. [4] and Mushtaq et al. [19]. As far as medium scale production using deuterons is concerned, only Mushtaq et al. [19] measured the integral yield of ^{73}Se after irradiations with a beam current

of 2 μA. It amounted to about 68% of the theoretical value and the levels of ^{72}Se and ^{75}Se were low (see Table 5). No real high-current production experiment has been reported for ^{72}Se and ^{75}Se. From the evaluated data presented in this work, the ^{75}As(d,2n)^{72}Se reaction appears to be viable for the production of ^{75}Se. However, for the production of ^{72}Se, no statement can be made because the energy range covered so far is too low and the cross section is still rising in the early part of the excitation function.

7 Comparison of production routes

A comparison of the calculated yields of ^{73}Se via the reactions ^{75}As(p,3n)^{75}Se and ^{75}As(d,4n)^{73}Se is given in Figure 13. Evidently, the ^{75}As(p,3n)^{73}Se reaction gives a higher rate of production over the whole energy range. Furthermore, the ^{72,75}Se impurity level is <0.1%. Therefore, the ^{75}As(p,3n)^{73}Se reaction has been extensively used for the production of ^{73}Se [4–6, 18–20]. The high-energy reaction ^{nat}Br(p,x)^{73}Se over $E_p = 100 \rightarrow 69$ MeV also gives a good yield of ^{73}Se (263 MBq/μAh) but not as high as the (p,3n) and (d,4n) reactions on ^{75}As. Also, the ^{72,75}Se impurity level in high energy reaction is about 3% [22]. It is therefore not often used for the production of ^{73}Se.

A comparison of the calculated yields of ^{75}Se via the ^{75}As(p,n)^{75}Se and ^{75}As(d,2n)^{75}Se reactions is given in Figure 14. Evidently, upto 20 MeV, the proton induced reaction has a higher yield, but beyond that energy the yield of the (d,2n) reaction becomes much higher. In practice, the (p,n) reaction has been extensively used for the production of ^{75}Se [4–6, 21] because proton beams of about 18 MeV are more commonly available than the deuteron beam. Again the high-energy ^{nat}Br(p,x)^{73}Se reaction is also interesting [22] but the level of the ^{72}Se impurity amounts up to 80%.

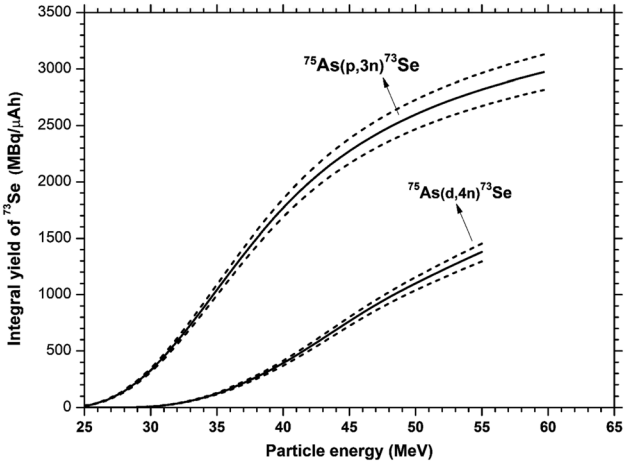

Figure 13: Comparison of integral yields of ^{73}Se from ^{75}As(p,3n)^{73}Se and ^{75}As(d,4n)^{73}Se reactions for 1 h irradiations. Some measured yields are also shown.

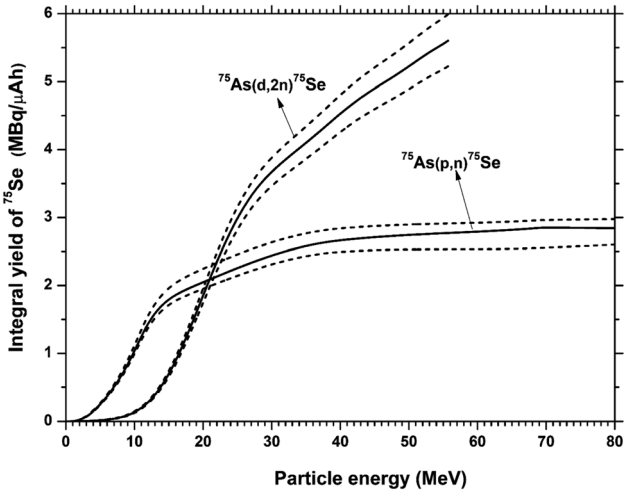

Figure 14: Comparison of integral yields of ^{75}Se from ^{75}As(p,n)^{75}Se and ^{75}As(d,2n)^{75}Se reactions for 1 h irradiations. Some measured yields are also shown.

As regards the production of ^{72}Se, the present choice lies on the ^{75}As(p,4n)^{72}Se reaction [13] because no data exist on the ^{75}As(d,5n)^{72}Se reaction beyond 55 MeV. The high-energy route ^{nat}Br(p,x)^{72}Se using $E_p = 92 \rightarrow 72$ MeV leads to a high yield of ^{72}Se [12] but it contains about 1.5 times more ^{75}Se. Although for the preparation of the ^{72}Se/^{72}As generator the large amount of ^{75}Se may not be a very serious problem, yet the ^{75}As(p,4n)^{72}Se reaction offers the possibility of obtaining ^{72}Se with the ^{75}Se impurity level limited to about 5% [13].

8 Conclusion

A critical analysis and evaluation of the cross section data of proton and deuteron induced nuclear reactions on ^{75}As leading to the formation of the three important radionuclides of selenium, namely ^{75}Se, ^{73}Se and ^{72}Se, showed that the proton induced reactions are most suitable for the production of those radionuclides with high radionuclidic purity. Whereas the longer lived ^{75}Se, important for tracer studies using SPECT, can be produced at a small-sized cyclotron via the ^{75}As(p,n)^{75}Se reaction using the energy range $E_p = 18 \rightarrow 8$ MeV, for the production of the other two radionuclides high energy protons are needed. The optimum energy range for the production of the non-standard positron emitter ^{73}Se via the ^{75}As(p,3n)^{73}Se reaction is $E_p = 40 \rightarrow 30$ MeV; the yield of ^{73}Se is high and the experimentally determined level of the ^{72,75}Se impurity amounts

to <0.1%. The useful energy range for the production ^{72}Se, a parent of the positron-emitting ^{72}Se/^{72}As generator system, via the ^{75}As(p,4n)^{72}Se reaction is E_p = 60 → 45 MeV; the yield is high and the level of the ^{75}Se impurity is <5%. The evaluated data, however, also suggest that for the production of those three radionuclides, the deuteron induced reactions on ^{75}As could also be used. The yields are lower and the impurities somewhat higher; nonetheless, the products may be acceptable for the desired applications.

Acknowledgments: N. Amjed would like to thank the Higher Education Commission of Pakistan (HEC) for the financial assistance. The work was done in the frame of HEC; NRPU project No. 9746.

Author contributions: All the authors have accepted responsibility for the entire content of this submitted manuscript and approved submission.

Research funding: This work was funded by Higher Education Commission of Pakistan (HEC), NRPU project No. 9746.

Conflict of interest statement: The authors declare no conflicts of interest regarding this article.

References

1. Ekambaramgnanadesigan B. K., Gnanagurudasan E., Santhosh K. N. A systematic review of selenium and its role in human reproductive system. *Int. J. Pharma Bio Sci.* 2013, *4*, B1.
2. Jereb M. Radiation dose to the human body from intravenuously administered ^{75}Se-sodium selenite. *J. Nucl. Med.* 1975, *16*, 846–850.
3. Paterson A. H. G., McCready V. R. *Clinical and Experimental Studies of Selenium-75-Labeled Compounds is Compared and Contrasted with Tumour Imaging by Means of ^{67}Ga-citrate*; IAEA, 1976; pp. 63–67.
4. Königs U., Humpert S., Spahn I., Qaim S. M., Neumaier B. Isolation of high purity ^{73}Se using solid phase extraction after selective 4,5-[^{73}Se]benzopiazselenol formation with aminonaphthalene. *Radiochim. Acta* 2018, *106*, 497–505.
5. Ermert J., Blum T., Hamacher K., Coenen H. H. Alternative syntheses of [$^{73,\ 75}$Se]selenoethers exemplified for homocysteine [$^{73,\ 75}$Se]selenolactone. *Radiochim. Acta* 2001, *89*, 863.
6. Helfer A., Ermert J., Humpert S., Coenen H. H. No-carrier-added labeling of the neuroprotective Ebselen with selenium-73 and selenium-75. *J. Label. Compd. Radiopharm.* 2015, *58*, 141–151.
7. Qaim S. M. Development of novel positron emitters for medical applications: nuclear and radiochemical aspects. *Radiochim. Acta* 2011, *99*, 611–625.
8. Qaim S. M., Scholten B., Spahn I., Neumaier B. Positron-emitting radionuclides for applications with special emphasis on their production methodologies for medical use. *Radiochim. Acta* 2019, *107*, 1011–1026.
9. Al-Kouraishi S. H., Boswell G. G. J. An isotope generator for ^{72}As. *Int. J. Appl. Radiat. Isot.* 1978, *29*, 607–609.
10. Phillips D. R., Hamilton V. T., Nix D. A., Taylor W. A., Jamriska D. J., Staroski R. C., Lopez R. A., Emran A. M. Chemistry and concept for an automated ^{72}Se/^{72}As generator. In *New Trends in Radiopharmaceutical Synthesis, Quality Assurance, and Regulatory Control*; Springer: Boston, MA, 1991; pp. 173–182. https://doi.org/10.1007/978-1-4899-0626-7_18.
11. Jennewein M., Qaim S. M., Kulkarni P., Mason R., Hermanne A., Roesch F. A no-carrier-added ^{72}Se/^{72}As radionuclide generator based on solid phase extraction. *Radiochim. Acta* 2005, *93*, 579–583.
12. Ballard B., Wycoff D., Birnbaum E. R., John K. D., Lenz J. W., Jurisson S. S., Cutler C. S., Nortier F. M., Taylor W. A., Fassbender M. E. Selenium-72 formation via ^{nat}Br(p,x) induced by 100 MeV protons: steps towards a novel ^{72}Se/^{72}As generator system. *Appl. Radiat. Isot.* 2012, *70*, 595–601.
13. DeGraffenreid A. J., Medvedev D. G., Phelps T. E., Gott M. D., Smith S. V., Jurisson S. S., Cutler C. S. Cross-section measurements and production of ^{72}Se with medium to high energy protons using arsenic containing targets. *Radiochim. Acta* 2019, *107*, 279–287.
14. NuDat 2.8. Data source National Nuclear Data Center, Brookhaven National Laboratory, based on ENSDF and the Nuclear Wallet Cards. http://www.nndc.bnl.gov/nudat2.
15. Hara T., Tilbury R. S., Fareed B. R. Production of ^{73}Se in cyclotron and its uptake in tumors of mice. *Int. J. Appl. Radiat. Isot.* 1973, *24*, 377–384.
16. Mushtaq A., Qaim S. M. Excitation functions of α-and ^{3}He-particle induced nuclear reactions on natural germanium: evaluation of production routes for ^{73}Se. *Radiochim. Acta* 1990, *50*, 27–32.
17. Blessing G., Lavi N., Qaim S. M. Production of ^{73}Se via the ^{70}Ge (α,n)-process using high current target materials. *Appl. Radiat. Isot.* 1992, *43*, 455–461.
18. Nozaki T., Itoh Y., Ogawa K. Yield of ^{73}Se for various reactions and its chemical processing. *Int. J. Appl. Radiat. Isot.* 1979, *30*, 595–599.
19. Mushtaq A., Qaim S. M., Stöcklin G. Production of ^{73}Se via (p,3n) and (d,4n) reactions on arsenic. *Appl. Radiat. Isot.* 1988, *39*, 1085–1091.
20. Plenevaux A., Guillaume M., Brihaye C., Lemaire C., Cantineau R. Chemical processing for production of no-carrier-added selenium-73 from germanium and arsenic targets and synthesis of l-2-amino-4-([^{73}Se]methylseleno) butyric acid (l-[^{73}Se] selenomethionine). *Appl. Radiat. Isot.* 1990, *41*, 829.
21. Blessing G., Lavi N., Hashimoto K., Qaim S. M. Thermochromatographic separation of radioselenium from irradiated Cu_3As-target: production of no-carrier added ^{75}Se. *Radiochim. Acta* 1994, *65*, 93–98.
22. Faßbender M., de Villiers D., Nortier M. F., van der Walt N. The ^{nat}Br(p,x)^{73,75}Se nuclear processes: a convenient route for the production of radioselenium tracers relevant to amino acid labelling. *Appl. Radiat. Isot.* 2001, *54*, 905.
23. Brodovitch J. C., Hogan J. J., Burns K. I. The pre-equilibrium statistical model: comparison of calculation with two (p,xn) reactions. *J. Inorg. Nucl. Chem.* 1976, *38*, 1581–1586.
24. Qaim S. M., Mushtaq A., Uhl M. Isomeric cross-section ratio for the formation of $^{73\ m,g}$Se in various nuclear processes. *Phys. Rev. C Nucl. Phys.* 1988, *38*, 645.
25. Levkovskij V. N. *Activation Cross Section of Nuclides of Average Masses (A= 40-100) by Protons and Alpha-Particles with Average Energies (E= 10-50 MeV)*; Intervesi: Moscow, USSR, 1991.

26. Albert R. (p, n) cross section and proton optical-model parameters in the 4- to 5.5-MeV energy region. *Phys. Rev.* 1959, *115*, 925–927.
27. Delaunay-Olkowsky J., Strohal P., Cindro N. Total reaction cross sections of proton induced reactions. *Nucl. Phys.* 1963, *47*, 266–272.
28. Johnson C. H., Trail C. C., Galonsky A. Thresholds for (p,n) reactions on 26 intermediate-weight nuclei. *Phys. Rev.* 1964, *136 B*, 1719–1729.
29. Johnson C. H., Galonsky A., Ulrich J. P. Proton strength functions from (p,n) cross sections. *Phys. Rev.* 1958, *109*, 1243.
30. Röhm H. F., Münzel H. Excitation functions for deuteron reactions with ^{75}As. *J. Inorg. Nucl. Chem.* 1972, *34*, 1773–1784.
31. Qaim S. M. Nuclear data relevant to cyclotron produced short-lived medical radioisotopes. *Radiochim. Acta* 1982, 147–162.
32. Qaim S. M. Nuclear data for production and medical application of radionuclides: present status and future needs. *Nucl. Med. Biol.* 2017, *44*, 31–49.
33. Qaim S. M., Spahn I., Scholten B., Neumaier B. Uses of alpha particles, especially in nuclear reaction studies and medical radionuclide production. *Radiochim. Acta* 2016, *104*, 601–624.
34. Qaim S. M., Spahn I. Development of novel radionuclides for medical applications. *J. Label. Compd. Radiopharm.* 2018, *61*, 126–140.
35. Tárkányi F., Ignatyuk A. V., Hermanne A., Capote R., Carlson B. V., Engle J. W., Verpelli M., Kellett M. A., Kibedi T., Kim G. N., Kondev F. G., Hussain M. Recommended nuclear data for medical radioisotope production: diagnostic positron emitters. *Nucl. Chem.* 2019, *319*, 533–666.
36. Hermanne A., Ignatyuk A. V., Capote R., Carlson B. V., Engle J. W., Kellett M. A., Kibédi T., Kim G., Kondev F. G., Hussain M. Reference cross sections for charged-particle monitor reactions. *Nucl. Data Sheets* 2018, *148*, 338–382.
37. RIPL-3 d. International Atomic Energy Agency, Vienna. www.nds-iaea.org/RIPL-3/.
38. Amjed N., Hussain M., Aslam M. N., Tárkányi F., Qaim S. M. Evaluation of nuclear reaction cross sections for optimization of production of the emerging diagnostic radionuclide ^{55}Co. *Appl. Radiat. Isot.* 2016, *108*, 38–48.
39. Amjed N., Wajid A. M., Ahmad N., Ishaq M., Aslam M. N., Hussain M., Qaim S. M. Evaluation of nuclear reaction cross sections for optimization of production of the important non-standard positron emitting radionuclide ^{89}Zr using proton and deuteron induced reactions on ^{89}Y target. *Appl. Radiat. Isot.* 2020, *165*, 1–9.
40. Dityuk A. I., Konobeyev A. Y., Lunev V. P., Shubin Y. N. *New Advanced Version of Computer Code ALICE-IPPE*. IAEA: Vienna. Report. INDC(CCP)-410, 1998.
41. Bojowald J., Machner H., Nann H., Oelert W., Rogge M., Turek P. Elastic deuteron scattering and optical model parameters at energies up to 100 MeV. *Phys. Rev.* ***C*** 1988, *38*, 1153–1163.
42. Morillon B., Romain P. Bound single-particle states and scattering of nucleons on spherical nuclei with a global optical model. *Phys. Rev. C* 2007, *76*, 044601.
43. Koning A. J., Delaroche J. P. Local and global nucleon optical models from 1 keV to 200 MeV. *Nucl. Phys. A* 2003, *713*, 231–310.
44. Koning A. J., Rochman D. Modern nuclear data evaluation with the TALYS code system. *Nucl. Data Sheets* 2012, *113*, 2841–2934.
45. Perey C. M., Perey F. G. Deuteron optical model analysis in the range of 11 to 27 MeV. *Phys. Rev.* 1963, *132*, 755–773.
46. Qaim S. M., Sudár S., Scholten B., Koning A. J., Coenen H. H. Evaluation of excitation functions of ^{100}Mo(p,d+pn)^{99}Mo and ^{100}Mo(p,2n)^{99m}Tc reactions: estimation of long-lived Tc-impurity and its implication on the specific activity of cyclotron-produced ^{99m}Tc 101-113. *Appl. Radiat. Isot.* 2014, *85*, 101–113.
47. Qaim S. M. Nuclear data for medical applications: an overview. *Radiochim. Acta* 2001, *89*, 189–196.
48. Otuka N., Takacs S. Definitions of radioisotope thick target yields. *Radiochim. Acta* 2015, *103*, 1–6.
49. Dmitriev P. P. *Radionuclide Yield in Reactions with Protons, Deuterons, Alpha Particles and Helium-3: Handbook*. IAEA: Vienna. Report. INDC(CCP)-263, 1986.
50. Rowshanfarzad P., Jalilian A. R., Sabet M. Simultaneous production and quality control of ^{73}Se and ^{75}Se radioisotopes in a 30 MeV cyclotron. *Iran. J. Radiat. Res.* 2004, *2*, 1–7.
51. Qaim S. M. Medical radionuclide production-science and technology. De Gruyter Berlin/Boston 2019. https://doi.org/10.1515/9783110604375.